Oncology Research, Vol. 28, pp. 857–872
Printed in the USA.

0965-0407/22 $90.00 + .00
DOI: https://doi.org/10.3727/096504021X16203818567367
E-ISSN 1555-3906
www.cognizantcommunication.com

lncCRLA Enhanced Chemoresistance in Lung Adenocarcinoma That Underwent Epithelial–Mesenchymal Transition

Weili Min,*[1] Liangzhang Sun,†[1] Burong Li,‡ Xiao Gao,* Shuqun Zhang,* and Yang Zhao*

*Department of Oncology, the Second Affiliated Hospital of Xi'an Jiaotong University, Xi'an, P.R. China
†Thoracic Department, the Second Affiliated Hospital of Xi'an Jiaotong University, Xi'an, P.R. China
‡Department of Clinical Laboratory, the Second Affiliated Hospital of Xi'an Jiaotong University, Xi'an, P.R. China

EMT confers increased metastatic potential and the resistance to chemotherapies to cancer cells. However, the precise mechanisms of EMT-related chemotherapy resistance remain unclear. c-Src-mediated caspase 8 phosphorylation essential for EMT in lung adenocarcinoma cell lines preferentially occurs in cells with the mesenchymal phenotype, resulting in chemoresistance to cisplatin plus paclitaxel in patients with resectable lung adenocarcinoma and a significantly worse 5-year PFS. Cisplatin killed lung adenocarcinoma cells regardless of caspase 8. Paclitaxel-triggered necroptosis in lung adenocarcinoma cells was dependent on the phosphorylation or deficiency of caspase 8, during which FADD interacted with RIPK1 to activate the RIPK1/RIPK3/MLKL signaling axis. Accompanied with c-Src-mediated caspase 8 phosphorylation to trigger EMT, a novel lncRNA named lncCRLA was markedly upregulated and inhibited RIPK1-induced necroptosis by impairing RIPK1–RIPK3 interaction via binding to the intermediate domain of RIPK1. Dasatinib mitigated c-Src-mediated phosphorylation of caspase 8-induced EMT and enhanced necroptosis in mesenchymal-like lung adenocarcinoma cells treated with paclitaxel, while c-FLIP knockdown predominantly sensitized the mesenchymal-like lung adenocarcinoma cells to paclitaxel + dasatinib. c-Src–caspase 8 interaction initiates EMT and chemoresistance via caspase 8 phosphorylation and lncCRLA expression, to which the dasatinib/paclitaxel liposome + siFLIP regimen was lethal.

Key words: Epithelial–mesenchymal transition (EMT); Chemotherapy resistance; Lung adenocarcinoma; Long noncoding RNAs (lncRNAs)

INTRODUCTION

In both the US and P.R. China, lung cancer is not only the leading cause of cancer death by far but also the second leading cause of death from any cause after heart disease based on calculations from published data[1,2]. Non-small cell lung cancer (NSCLC) accounts for approximately 85% of lung cancers with a markedly increased incidence of lung adenocarcinoma[3]. The 5-year overall survival rate for lung adenocarcinoma is only 17% because, in a startlingly high proportion of patients with lung adenocarcinoma, the disease has already metastasized at the initial diagnosis or recurs after initial surgery or radiotherapy[4,5]. Lung adenocarcinoma is generally incurable because it will either have an intrinsic resistance to chemotherapy or develop acquired resistance after an initial response[6,7]. Therefore, identifying molecular determinants of the resistance to chemotherapy in lung adenocarcinoma is necessary to improve its clinical efficacy.

Despite significant advances in diagnosing and treating lung adenocarcinoma, metastasis persists as a barrier to successful treatment and the main cause of cancer-related death[8–10]. Epithelial–mesenchymal transition (EMT), wherein epithelial cells depolarize, lose their cell–cell contacts, and gain an elongated, fibroblast-like morphology, is a potential mechanism by which tumor cells acquire metastatic features[11,12]. The prometastatic role of EMT in various human cancers was recently challenged by the research groups of Kari R. Fischer and Xiaofeng Zheng, who both stated that EMT was not a rate-limiting step for metastasis but rather inadvertently conferred resistance to antiproliferative drugs such as gemcitabine[6,13]. Notwithstanding, EMT-induced resistance to antitumor drugs remains an integral characteristic of lung adenocarcinoma. We observed that phosphorylation of caspase 8 by

[1]These authors provided equal contribution to this work.
Address correspondence to Yang Zhao, M.D., Department of Oncology, the Second Affiliated Hospital of Xi'an Jiaotong University, No. 157 Fifth West Road, Xi'an, Shaanxi Province 710004, P.R. China. Tel: +86 29 87679512; E-mail: szhaoy@126.com

c-Src induced both EMT through c-Src overactivation and resistance to chemotherapy through necroptosis[14]. Hence, the mechanism by which phosphorylated caspase 8 confers resistance to chemotherapy appeared to be worth pursuing. In our study, c-Src-mediated caspase 8 phosphorylation essential for the EMT in lung adenocarcinoma cell lines was preferential for the mesenchymal phenotype, leading to chemoresistance to cisplatin plus paclitaxel in patients with resectable lung adenocarcinoma. Cisplatin rendered lung adenocarcinoma cells susceptible to death regardless of caspase 8, while the paclitaxel-triggered necroptosis in lung adenocarcinoma cells was dependent on the phosphorylation or deficiency of caspase 8. During this necroptosis activation, FADD interplayed with RIPK1 to activate the RIPK1/RIPK3/MLKL signaling axis. Concomitant with c-Src-mediated caspase 8 phosphorylation to trigger EMT, a brand new lncRNA, named lncCRLA (chemotherapy resistance in lung adenocarcinoma), was markedly upregulated to inhibit RIPK1-induced necroptosis by impairing of the RIPK1–RIPK3 interaction via binding to the intermediate domain (ID) of RIPK1. Dasatinib, a c-Src inhibitor, impaired c-Src-mediated phosphorylation of caspase 8-induced EMT and enhanced necroptosis in paclitaxel-treated mesenchymal-like lung adenocarcinoma cells. Intriguingly, c-FLIP knockdown predominantly sensitized the mesenchymal-like lung adenocarcinoma cells to paclitaxel + dasatinib.

MATERIALS AND METHODS

Ethics Approval and Consent to Participate

The procedures of this study, including seven references, were approved by the Ethics Committee of the Second Affiliated Hospital of Xi'an Jiaotong University. The experiments were performed upon receiving written consent from each subject. The study methodologies conformed to the standards set by the Declaration of Helsinki.

Reagents and Drugs

Paclitaxel (Bristol-Myers Squibb, New York, NY, USA) was purchased from Sigma-Aldrich (Shanghai, P.R. China) for cell culture and animal studies at concentrations of 100, 200, and 400 nM. An original solution of cisplatin (Pfizer, New York, NY, USA) at a concentration of 1 M was stored at 4°C and freshly dissolved in culture medium before use. Dasatinib (Bristol-Myers Squibb) was dissolved in dimethyl sulfoxide (DMSO) and used at a final concentration of 10^{-6} M. z-VAD-fmk (50 mM) and z-IETD-fmk (50 mM) were obtained from Alexis Biochemicals. 3-Methyladenine (3-MA; 1 mg/10 ml) was purchased from InvivoGen (Hong Kong, China). Necrostatin-1 (nec-1; 10 mM) was generously gifted by Chen Huang from the Department of Cell Biology, Xi'an Jiaotong University, Shaanxi Province, P.R. China.

Cell Culture, DNA/Short Hairpin RNA (shRNA) Transfection, and Stable Cell Line Generation

Lung adenocarcinoma cell lines, including A549, National Cancer Institute (NCI)-H522, and H23, were gifts from Chen Huang from the Department of Cell Biology, Xi'an Jiaotong University (Shaanxi Province, P.R. China). H1395, H1437, H1573, H920, H2935, H1650, H1299, H2030, H2405, H647, and H838 cells were purchased from the American Type Culture Collection (ATCC; Manassas, VA, USA) and cultured in RPMI-1640 supplemented with 10% fetal bovine serum (FBS; HyClone, Logan, UT, USA) and penicillin/streptomycin/L-glutamine (Sigma-Aldrich). The cell lines in our study were authenticated by short tandem repeat (STR) analysis. To observe the morphologic features of EMT, we cultured cells for 5 days on fibronectin (10 μg/ml)-coated dishes. Cells were assayed for expression and viability following treatment with reagents or drugs at 2 days after attachment to the fibronectin-coated dishes. Knockdown of RIPK1, FADD, c-FLIP, caspase 8, c-Src, or lncCRLA was performed using lentivirus-delivered shRNAs constructed by GenePharma [shRNAs targeting c-FLIP and lncCRLA corresponded to the small interfering RNA (siRNAs) below; Shanghai, P.R. China]. Following lentiviral transfection, stable cell lines were selected via culturing in the presence of 500 μg/ml G418 (Gibco, ThermoFisher Scientific, Waltham, MA, USA). The open reading frames of genes of interest, including wild-type caspase 8, wild-type RIPK1, death domain-deleted RIPK1, ID-deleted RIPK1, kinase domain (KD)-deleted RIPK1, c-Src, and constitutively active c-Src (Src Y527F), were cloned into the MSCV-IRES-zeo plasmid with a hemagglutinin (HA) tag to allow the expression of HA-tagged proteins. The subsequent DNA was transfected into packaging cells. Virus-containing supernatants were removed, and debris was pelleted by centrifugation. Target cells were cultured in virus-containing supernatants for 48 h before selection for a stable cell line with 10 mg/ml zeocin (Invitrogen, ThermoFisher Scientific) for 14 days.

RESULTS

c-Src-Induced Caspase 8 Phosphorylation Was Required for EMT in Lung Adenocarcinoma Cell Lines

In lung adenocarcinoma, the molecular characteristics of EMT could be divided into the mesenchymal, epithelial, and intermediate phenotypes based on the expression of E-cadherin (E-cad) and vimentin (Vim)[15]. We distinguished lung adenocarcinoma cell lines as the epithelial or mesenchymal properties (described as epithelial-like and mesenchymal-like cells, respectively). Prior work showed that phosphorylation of caspase 8 at tyrosine 380 (p-Casp8) by c-Src enhances c-Src activation (p-Src) and triggers EMT[14,16,17]. Thus, it was likely that p-Casp8

could function as a biomarker for EMT in lung adenocarcinoma. We initially investigated the expression levels of c-Src and caspase 8 in lung adenocarcinoma cells, which showed both proteins were ubiquitously expressed (Fig. 1A and B). However, caspase 8 expression was absent in H522 cells (Fig. 1A and B). p-Casp8 was present in the mesenchymal-like lung adenocarcinoma cell lines with lower E-cad levels and higher Vim levels (Fig. S1A), whereas no p-Casp8 was observed in the epithelial-like cell lines with higher E-cad levels and lower Vim levels (Fig. S1B). There was remarkably lower c-Src expression in the epithelial-like cell lines than in the mesenchymal-like cell lines (Fig. 1A and B). A549 cells transfected with control shRNA and H522 cells with ectopic expression of caspase 8 presented the mesenchymal-like morphology with E-cad downregulation and Vim upregulation (A549 + control/H522 + Casp8: mesenchymal-like) (Fig. 1C and D and Fig. S1C), whereas A549 cells with c-Src/caspase 8 knockdown and H522 cells transfected with control vector presented epithelial properties (A549 + Casp8/Src shRNA and H522 + control: epithelial-like) (Fig. 1C and D and Fig. S1C). Taken together, c-Src-induced caspase 8 phosphorylation was required for EMT in lung adenocarcinoma cell lines.

To further clarify the role of c-Src in EMT, we ectopically expressed c-Src in epithelial-like lung adenocarcinoma cell lines with caspase 8 expression (H1395, H1437, H1573, H1693, and H1568). The molecular and morphological characteristics in cells were more mesenchymal-like, while these changes were concomitant with markedly increased levels of p-Casp8 and p-Src in the epithelial-like lung adenocarcinoma cell lines transfected with c-Src (Fig. 1E and F and Fig. S1D). Furthermore, upregulation of c-Src induced more aggressive behavior in the epithelial-like cell lines (Fig. 1G and Fig. S1E and F). It was noteworthy that c-Src was mildly activated in H522 cells lacking caspase 8. The results suggested that the expression level of c-Src was associated with its basic activity to initiate caspase 8 phosphorylation in lung adenocarcinoma.

c-Src-Induced Caspase 8 Phosphorylation Was Associated With the Mesenchymal Phenotype and Contributed to Chemoresistance in Lung Adenocarcinoma

As the antiapoptotic role of p-Casp8 in several human tumors has been described[16], we sought to uncover the underlying mechanism by which p-Casp8-induced EMT restricted the clinical efficacy of the TP regimen in lung adenocarcinoma. It was a tremendous challenge to assess the epithelial/mesenchymal status of tumor tissues due to the heterogeneity in the diverse domains of the tumor.

According to our outcomes in a prior report[15,17], Vim and E-cad were confirmed as appropriate biomarkers to

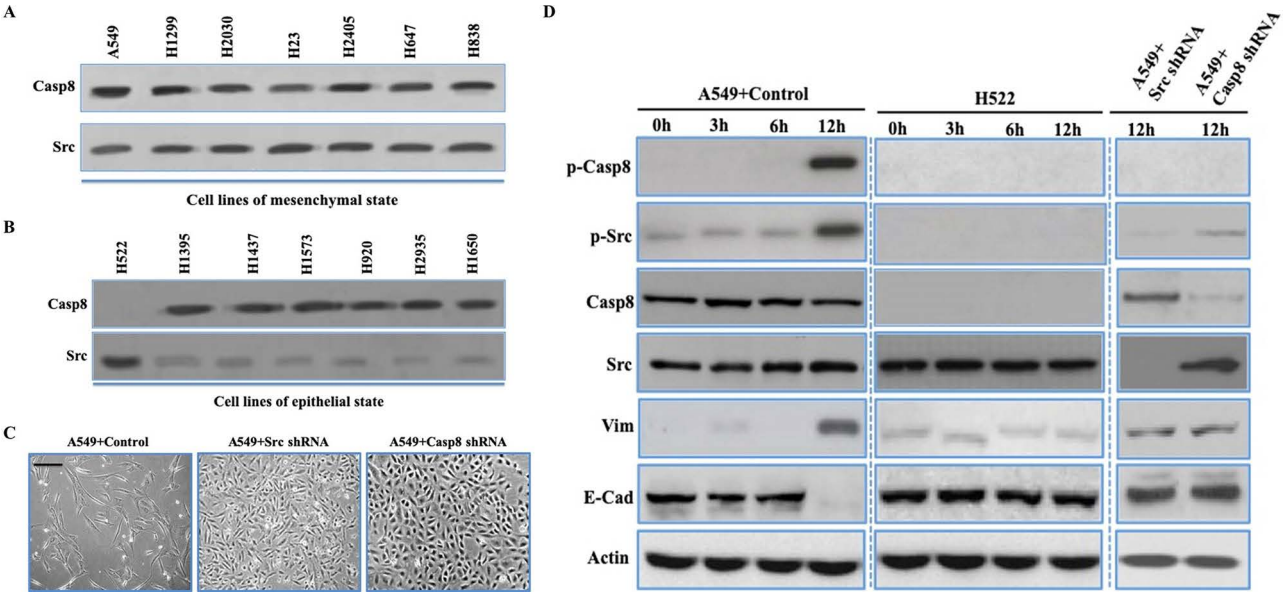

Figure 1. c-Src-induced caspase 8 phosphorylation was required for epithelial–mesenchymal transition (EMT) in lung adenocarcinoma cell lines. (A, B) Immunoblotting analysis of caspase 8 and c-Src in the mesenchymal-like (A) (A549, H1299, H2030, H23, H2405, H647, and H838) and epithelial-like (B) (H522, H1395, H1473, H1573, H920, and H1650) lung adenocarcinoma cell lines plated onto fibronectin for 5 days. (C) Phase contrast microscopy of A549 + control/c-Src/caspase 8 short hairpin RNA (shRNA) plated on dish coated with fibronectin over a 5-day period. Scale bars: 50 μm. (D) Immunoblotting analysis of p-Casp8, p-Src, caspase 8, c-Src, vimentin, E-cadherin, and β-actin in the A549 cells with control/c-Src/caspase 8 shRNA and H522 cells plated onto fibronectin at indicated times. $*p < 0.05$.

predict the epithelial/mesenchymal properties of lung adenocarcinoma tissues. We initially assessed the expressions of p-Casp8, Vim, and E-cad through immunohistochemistry (IHC) in 40 patients with operable lung adenocarcinoma (Fig. 2A–C and Table 1). p-Casp8 was tightly associated with upregulated Vim and downregulated E-cad expression with mesenchymal-like properties (Fig. S2A–C), indicating that p-Casp8 could serve as a biomarker for EMT in lung adenocarcinoma tissues.

We next investigated the relationship between p-Casp8 level and the response rate to neoadjuvant chemotherapy in patients with resectable lung adenocarcinoma. A total of 109 patients were divided into p-Casp8-positive (n = 52) and p-Casp8-negative (n = 57) groups (Table S1). Patients with p-Casp8-positive lung adenocarcinoma presented significantly lower complete response (CR) and partial response (PR) rates following two neoadjuvant cycles of the TP regimen (Fig. 2D). In addition to the lower response rate to the TP regimen, the p-Casp8-positive cohort exhibited a remarkably poorer 5-year progression-free survival (PFS) ($p < 0.05$) (Fig. 2E). Next, we recruited 20 patients with metastatic lung adenocarcinoma to examine the levels of p-Casp8. As shown in Table S2, patients with p-Casp8-negative lung adenocarcinoma exhibited a better response to the TP regimen than did patients with p-Casp8-positive lung adenocarcinoma. Based on computed tomography (CT) images, there was a significant reduction in lesion size in the p-Casp8-negative group (Fig. S2D and E). Then seven pairs of pretreatment and posttreatment biopsies were acquired, and we detected markedly increased p-Casp8 following two cycles of the TP regimen (Fig. S2F). Moreover,

Table 1. Phosphorylated Caspase-8 and Clinical Characteristics in Patients With Resectable Lung Adenocarcinoma (N = 40)

	pY380-Casp8 [n (%)]		
	Positive	Negative	p Value
Age			<0.05
≤60	8 (44.4%)	6 (27.3%)	
>60	10 (55.6%)	16 (72.7%)	
Gender			>0.05
Male	12 (66.7%)	15 (68.2%)	
Female	6 (33.3%)	7 (31.8%)	
Differentiation			>0.05
Well	3 (16.7%)	4 (18.2%)	
Moderate	5 (27.8%)	5 (22.7%)	
Poor	10 (55.5%)	13 (58.8%)	
Lymphonode			>0.05
N0-1	7 (38.9%)	9 (40.9%)	
N2-3	11 (61.1%)	13 (59.1%)	
pTNM			<0.05
I–II	4 (22.2%)	9 (40.9%)	
III–IV	14 (77.8%)	13 (59.1%)	
Radiotherapy	12 (66.7%)	16 (72.7%)	>0.05

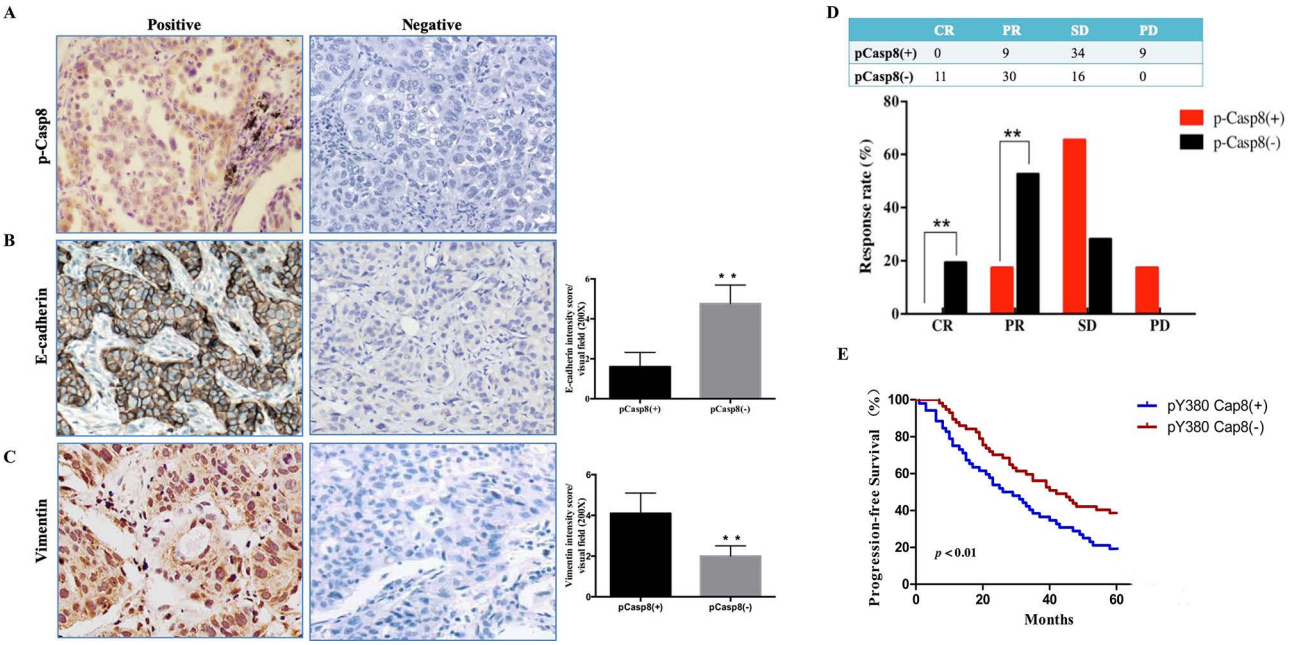

Figure 2. c-Src-induced caspase 8 phosphorylation was associated with the mesenchymal phenotype and contributed to chemoresistance in lung adenocarcinoma. (A–C) Immunohistochemical stainings for p-Casp8 (A), E-cadherin (B), and vimentin (C) with high magnification (400×). $^{**}p < 0.01$. (D) Response to cisplatin plus paclitaxel of patients with resectable lung adenocarcinoma. $^{**}p < 0.01$. (E) Kaplan–Meier progression-free survival (PFS) curve for 109 lung adenocarcinoma patients with p-Casp8(+) or p-Casp8(−) following two neoadjuvant cycles of cisplatin and paclitaxel.

the proportion of p-Casp8-positive cells was sharply increased following TP regimen treatment (Fig. S2G). Taken together, the results showed that in lung adenocarcinomas, p-Casp8 was associated with mesenchymal-like properties and contributed to disease progression by increasing the resistance to the TP regimen.

c-Src-Mediated Caspase 8 Phosphorylation Inhibited Cell Death of Lung Adenocarcinoma Through the Paclitaxel-Triggered Necroptosis During EMT

Next, we sought to determine the underlying mechanism for the difference in response to the TP regimen in p-Casp8-positive and p-Casp8-negative lung adenocarcinoma. A549 cells were stably transfected with lentiviral control, caspase 8, or c-Src shRNA (A549 + control: mesenchymal-like; A549 + caspase 8/c-Src shRNA: epithelial-like). Cisplatin caused A549 cell death in a time- and concentration-dependent manner regardless of c-Src or caspase 8 expression (Fig. 3A). Cisplatin might not contribute to resistance to the TP regimen in p-Casp8-positive lung adenocarcinoma. Comparing with the mesenchymal-like A549 cells, the antitumor efficacy of paclitaxel in A549 cells transduced with c-Src shRNA was most potent and was dependent on the intervention time and drug concentration (Fig. 3B), while caspase 8 knockdown in A549 cells strikingly yielded a marked increase in paclitaxel-mediated cell death (Fig. 3B). These data were further supported by in vivo xenograft and in vitro colony assays (Fig. S3A and B). Then we analyzed the response to the TP regimen in the lung adenocarcinoma tissues from p-Casp8-negative patients, who were divided into two groups according to IHC testing of caspase 8 and c-Src: Casp8(+)c-Src(−) (n = 20) and Casp8(−)c-Src(+) (n = 37) (Fig. S3C). The response to the TP regimen in Casp8(+)c-Src(−) patients was significantly superior to that in Casp8(−)c-Src(+) patients (Fig. S3D and E). It indicated that caspase 8 yielded more antitumor activities relative to phosphorylated or lacking caspase 8 in response to paclitaxel treatment in lung adenocarcinoma.

Paclitaxel interferes with mitotic spindle dynamics to induce an extended G_2/M arrest, which can lead to cell death[18]. Consistently, paclitaxel significantly enhanced G_2/M arrest of A549 cells (Fig. S3F). To decipher the paclitaxel-triggered tumoricidal mechanism in lung adenocarcinoma, the inhibitors specific for RIPK1-induced necroptosis (nec-1), caspase 8-induced apoptosis (z-IETD-fmk), pan-caspase-induced apoptosis (z-VAD-fmk), and autophagy (3-MA) were applied. As shown in Figure 3C, paclitaxel committed approximately 70% of c-Src-silenced A549 cells to death as indicated by a marked increase in the number of annexin V-positive cells (apoptotic cells) which was completely blocked by either z-IETD-fmk or z-VAD-fmk alone (Fig. 3C and Fig. S3G). Prior work reported that blocking caspase 8-induced apoptosis led to cell death dependent on RIPK1 and RIPK3, which was defined as necroptosis following sensing death[19,20]. Consistently, paclitaxel gave rise to a marked increase in the proportion of propidium iodide (PI)-positive cells (necrotic cells) in A549 cells transduced with caspase 8 shRNA (Fig. 3C), which was prevented by the addition of nec-1 (Fig. S3G). Notably, the mesenchymal-like A549 cells (A549 + control) with caspase 8 phosphorylation were resistant to paclitaxel-induced cell death. However, treatment with nec-1 restored a smaller amount of cell viability compared with that in A549 cells transduced with caspase 8 shRNA (Fig. 3B and C and Fig. S3G). The type of cell death, apoptosis or necroptosis, in the paclitaxel-treated A549 cells was identified by observing apoptotic or necrotic features under an electron microscope (Fig. 3D).

To extend our notion, we examined the mesenchymal-like and the epithelial-like lung adenocarcinoma cell lines. Paclitaxel was more lethal to the epithelial-like cell lines except for H522 cells, which naturally lacked caspase 8 (Fig. S3H). Nec-1 blocked the paclitaxel-induced cell death of mesenchymal-like cells (Fig. 3E), whereas z-IETD-fmk restored the viability of the epithelial-like cells (Fig. S3H). With the epithelial-like properties, caspase 8-deficient H522 cells showed cell death similar to A549 cells transduced with caspase 8 shRNA (Fig. S3H). In addition, autophagy might not influence either cisplatin- or paclitaxel-induced cell death (Fig. 3C). Taken together, caspase 8 phosphorylation or knockdown initiated the necroptosis of lung adenocarcinoma under paclitaxel treatment, whereas the mesenchymal-like A549 cells with control shRNA had considerable resistance to paclitaxel.

Our previous study revealed that phosphorylated caspase 8 by c-Src overactivated c-Src to phosphorylate E-cad phosphorylated by RNF43-initiated E-cad ubiquitination to maintain EMT in lung adenocarcinoma[17]. To dissect the relationship between EMT and resistance to chemotherapy, we stably transfected H522 cells with control vector, caspase 8 holoprotein or constitutively active c-Src (Src Y527F) (Fig. S3I)[21], and A549 cells with control or RNF43 shRNA (Fig. S3J), in which H522 cells expressing caspase 8/Src Y527F and A549 cells with RNF43 knockdown exhibited mesenchymal-like properties[17]. RNF43 knockdown impaired EMT without influencing the c-Src–caspase 8 interaction and promoted a marked increase in necroptotic cell death in A549 cells treated with paclitaxel (Fig. S3K). Intriguingly, the transfection of Src Y527F and caspase 8 into H522 cells facilitated EMT and obviously attenuated paclitaxel-induced cell death (Fig. 3K). Collectively, these data suggest that the induction of EMT based on c-Src–caspase 8 increased the resistance of lung adenocarcinoma to paclitaxel.

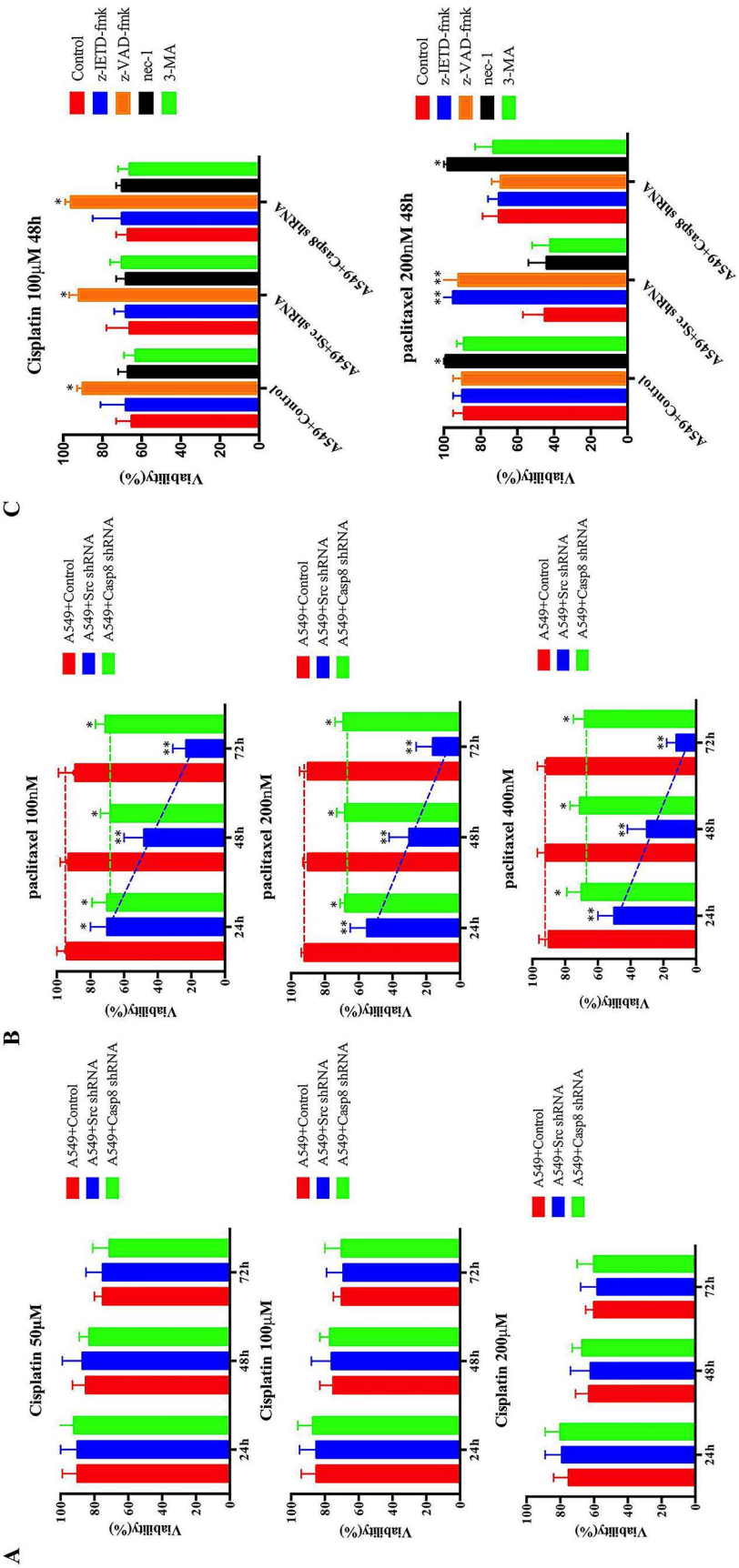

Figure 3. c-Src-mediated caspase 8 phosphorylation inhibited cell death of lung adenocarcinoma through the paclitaxel-triggered necroptosis during EMT. (A, B) A549 cells with control/c-Src/caspase 8 shRNA were treated with cisplatin (50/100/200 μM) (A) or paclitaxel (100/200/300 nM) (B) for 24, 48, and 72 h. Cell viability was determined by measuring ATP levels using Cell Titer-Glo kit. Data were represented as mean ± standard deviation of duplicates. $*p < 0.05$. $**p < 0.01$. (C) A549 cells with control/c-Src/caspase 8 shRNA was treated with cisplatin (100 μM, upper) or paclitaxel (200 nM, lower) with the addition of dimethyl sulfoxide (DMSO) (control), z-IETD-fmk (50 mM), z-VAD-fmk (50 mM), necrostatin-1 (nec-1) (10 mM), or 3-MA (25 mM) for 48 h. Cell viability was determined by measuring ATP levels using Cell Titer-Glo kit. Data were represented as mean ± standard deviation of duplicates. $*p < 0.05$. $**p < 0.01$.

FADD Interacted With Caspase 8, c-FLIP, and RIPK1 to Induce Cell Death Signaling Following Paclitaxel Treatment

Next, we determined the molecular mechanisms underlying the antitumor efficiency of paclitaxel. Paclitaxel triggered the apoptotic cleavage of caspase 8 in c-Src-silenced A549 cells (Fig. 4A). After we labeled tumor cells with [^{32}P]-orthophosphate, RIPK1, RIPK3, and MLKL were phosphorylated in A549 cells stably transfected with caspase 8 shRNA treated with paclitaxel (Fig.

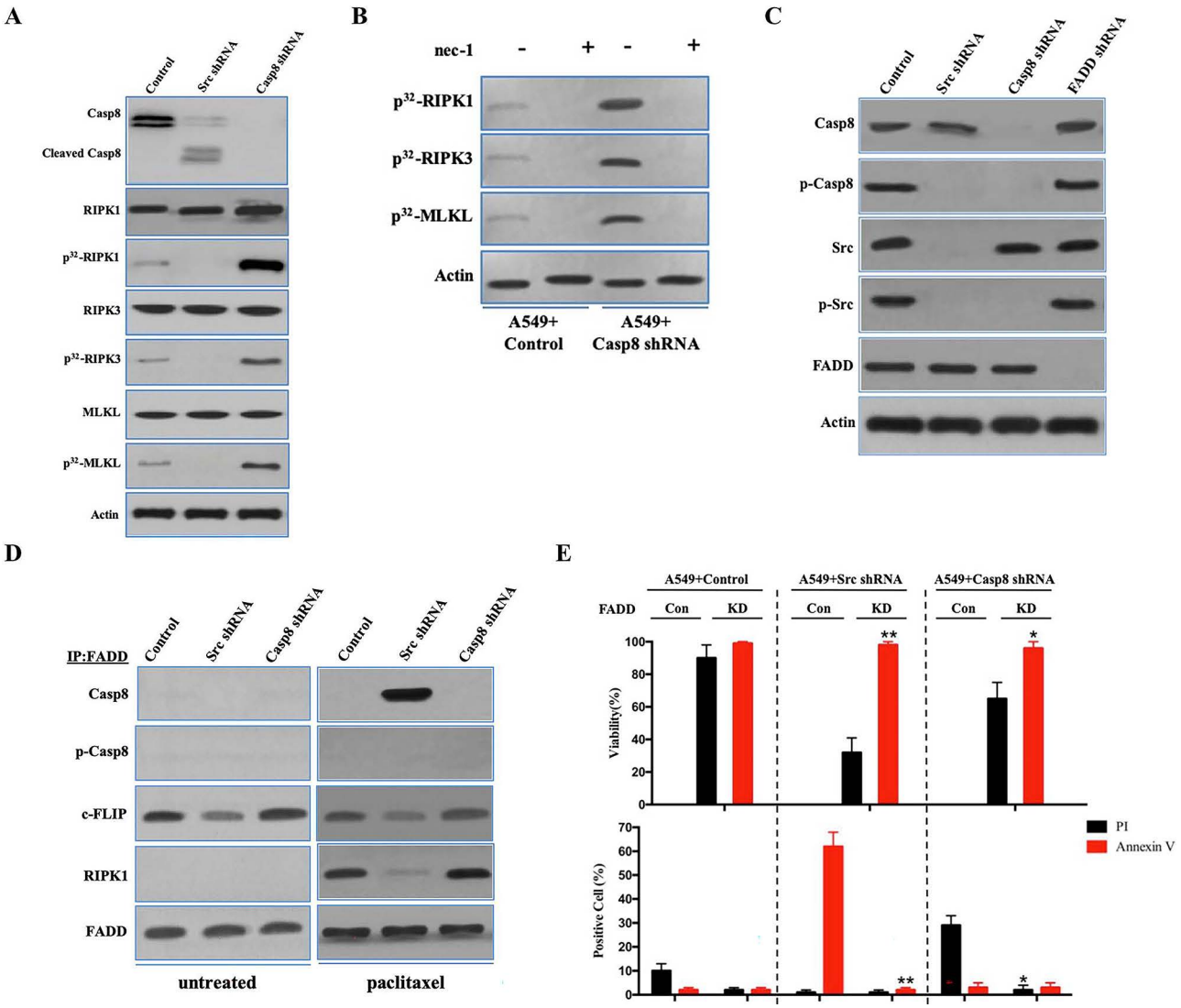

Figure 4. FADD interacted with caspase 8, c-FLIP, and RIPK1 to induce cell death signaling following paclitaxel treatment. (A) Immunoblotting analysis of caspase 8, cleaved caspase 8, RIPK1, RIPK3, MLKL, and β-actin in A549 cells with control/c-Src/caspase 8 shRNA treated by 200 nM paclitaxel for 48 h after 48-h attachment on the fibronectin-coated dish. Cells were labeled with [^{32}P]-orthophosphate. Phosphorylated RIPK1, RIPK3, and MLKL were measured by Cyclone Plus Phosphor Imager. (B) A549 cells with control/caspase 8 shRNA were treated by 200 nM paclitaxel with or without nec-1 for 48 h after 48-h attachment on the fibronectin-coated dish. Cells were labelled with [^{32}P]-orthophosphate. Phosphorylated RIPK1, RIPK3, and MLKL were measured by Cyclone Plus Phosphor Imager. (C) Immunoblotting analysis of caspase 8, p-Casp8, c-Src, p-Src, FADD, and β-actin in A549 cells with control/c-Src/caspase 8/FADD shRNA after 48-h attachment on the fibronectin-coated dish. (D) The immunocomplexes of A549 cells with control/c-Src/caspase 8 shRNA treated with or without 200 nM paclitaxel for 48 h after 48-h attachment on the fibronectin-coated dish were eluted with antibody against FADD, and whole elution was used to measure caspase 8, p-Casp8, c-FLIP, and RIPK1. (E) A549 cells with control/c-Src or caspase 8 shRNA combined with or without FADD knockdown were treated with 200 nM paclitaxel for 48 h. Cell viability was determined by measuring ATP levels using Cell Titer-Glo kit. Data were represented as mean ± standard deviation of duplicates. Cells were analyzed for annexin V/propidium iodide (PI) staining by flow cytometry. All experiments were repeated three times with similar results. *$p < 0.05$ versus control, **$p < 0.01$ versus control.

4A), whereas A549 cells transfected with control shRNA exhibited a reduction in RIPK1, RIPK3, and MLKL phosphorylation (Fig. 4A). H522 cells with control vector and ectopic expression of caspase 8 presented a similar outcome as A549 cells under paclitaxel treatment (Fig. S4A). To determine whether RIPK1 activation played an important role in the paclitaxel-induced necroptosis of lung adenocarcinoma, we applied the RIPK1 inhibitor nec-1 to paclitaxel-treated A549 and H522 cells. Nec-1 was able to block RIPK1/RIPK3/MLKL activation in A549 and H522 cells with caspase 8 deficiency or phosphorylation (Fig. 4B and Fig. S4B). In the absence of caspase 8, c-Src overactivation via the expression of constitutively active c-Src (Src Y527F) in H522 cells exhibiting EMT attenuated the necroptotic RIPK1/RIPK3/MLKL signaling (Fig. S4A). Collectively, it was plausible that the mesenchymal state of lung adenocarcinoma cells yielded the resistance to paclitaxel-induced necroptosis.

Previous work elucidated that FADD bound to caspase 8, cellular FLICE (FADD-like IL-1β-converting enzyme)-inhibitory protein (long) (c-FLIP), and RIPK1 through death effector domains (DEDs) or the death domain (DD) to trigger alternative cell death pathways, apoptosis, or necroptosis[14,22]. We investigated whether FADD was necessary to induce lung adenocarcinoma cell death through its interaction with caspase 8, c-FLIP, and RIPK1. FADD deletion had no effect on the c-Src–caspase 8 interaction (Fig. 4C). In untreated A549 and H522 cells, caspase 8 and RIPK1 did not coimmunoprecipitate with FADD, which was accompanied by frequent binding of c-FLIP to FADD (Fig. 4D and Fig. S4C). Caspase 8 binding to FADD resulted in remarkably decreased c-FLIP binding to trigger apoptotic cell death in the paclitaxel-treated A549 cells transduced with c-Src shRNA (Fig. 4C and D), whereas p-Casp8 was not bound to FADD in the paclitaxel-treated A549 and H522 cells (Fig. 4D and Fig. S4C). RIPK1 was significantly increased in the coimmunoprecipitated complex with an antibody specific for FADD in the paclitaxel-treated A549 and H522 cells with deficient or phosphorylated caspase 8 (Fig. 4D and Fig. S4C). We next determined how FADD affected paclitaxel-induced cell death. FADD silencing via lentiviral delivery of shRNA (Fig. S4D and E) was able to rescue A549 and H522 cells from paclitaxel-induced apoptosis or necroptosis (Fig. 4E and Fig. S4F). FADD silencing proficiently inhibited the phosphorylation of RIPK1, RIPK3, and MLKL in A549 cells transduced with control or caspase 8 shRNA (Fig. 4F) and the apoptotic cleavage of caspase 8 in A549 cells transduced with c-Src shRNA (Fig. S4G). Similarly, FADD knockdown ablated RIPK1/RIPK3/MLKL activation to block the necroptosis of H522 cells (Fig. 4G). The antitumor activity of FADD in the paclitaxel-induced cell death was confirmed by in vivo xenograft analysis (Fig. S4H and I). Taken together, it suggested that FADD promoted the paclitaxel-induced cell death of lung adenocarcinoma via the assembly of FADD–c-FLIP–caspase 8–RIPK1.

To evaluate the role of c-FLIP in paclitaxel-induced cell death, c-FLIP in A549 cells was knocked down with lentiviral shRNA (Fig. S4J). Surprisingly, c-FLIP knockdown did not alter the apoptosis and necroptosis in A549 cells (Fig. S4J and K). In the immunoprecipitated complex using FADD antibody in paclitaxel-treated A549 cells, c-FLIP knockdown did not affect the interaction between RIPK1/caspase 8 and FADD (Fig. S4L). Consistently, c-FLIP knockdown did not affect the paclitaxel-induced H522 cell death (Fig. S4M and N), while the interaction between FADD and RIPK1/caspase 8 was not affected by c-FLIP in H522 cells (Fig. S4O). These data indicated that c-FLIP might suppress apoptosis in untreated cells and does not affect cell death under paclitaxel treatment.

lncRNA-Related Chemotherapy Resistance in Lung Adenocarcinoma (lncCRLA) Inhibited RIPK1-Induced Necroptosis in the Mesenchymal-Like Lung Adenocarcinoma

Necroptosis was obviously attenuated in the mesenchymal-like lung adenocarcinoma cells under paclitaxel treatment compared with that in the epithelial-like lung adenocarcinoma cells. We explored whether EMT contributed to resistance to paclitaxel in lung adenocarcinoma. An antibody against β-catenin, 7A7, was delivered to block β-catenin nuclear translocation, which inhibits EMT with no effects on the c-Src–caspase 8 interaction[14]. 7A7 antibody delivery promoted necroptotic cell death with RIPK1/RIPK3/MLKL activation in A549 and H522 cells and had no effect on c-Src-induced caspase 8 phosphorylation (Fig. 5A and B and Fig. S5A). The transfection of constitutively active c-Src (Src Y527F) into caspase 8-deficient H522 cells promoted EMT[17] and reduced RIPK1-induced necroptosis (Fig. S4A). This finding suggested that EMT in lung adenocarcinoma obviously reduced paclitaxel-triggered necroptotic cell death in lung adenocarcinoma.

Mounting evidence has indicated that lncRNAs are critical for chemotherapy resistance in various human tumors[23,24]. In an attempt to identify the lncRNA(s) required for EMT-related resistance to paclitaxel in mesenchymal-like lung adenocarcinoma cells, we conducted two sequential rounds of screening (Fig. S5B). First, an lncRNA microarray was utilized to compare lncRNA expression profiles between the mesenchymal-like (A549 + control: mesenchymal) and the epithelial-like (A549 + caspase 8/c-Src shRNA: epithelial) A549 cells (Fig. 5C). The eight most differentially expressed lncRNAs (fold change >8-fold) (Fig. 5D and Table S3) were validated by quantitative reverse transcription polymerase chain reaction (qRT-PCR) in A549 cells and H522

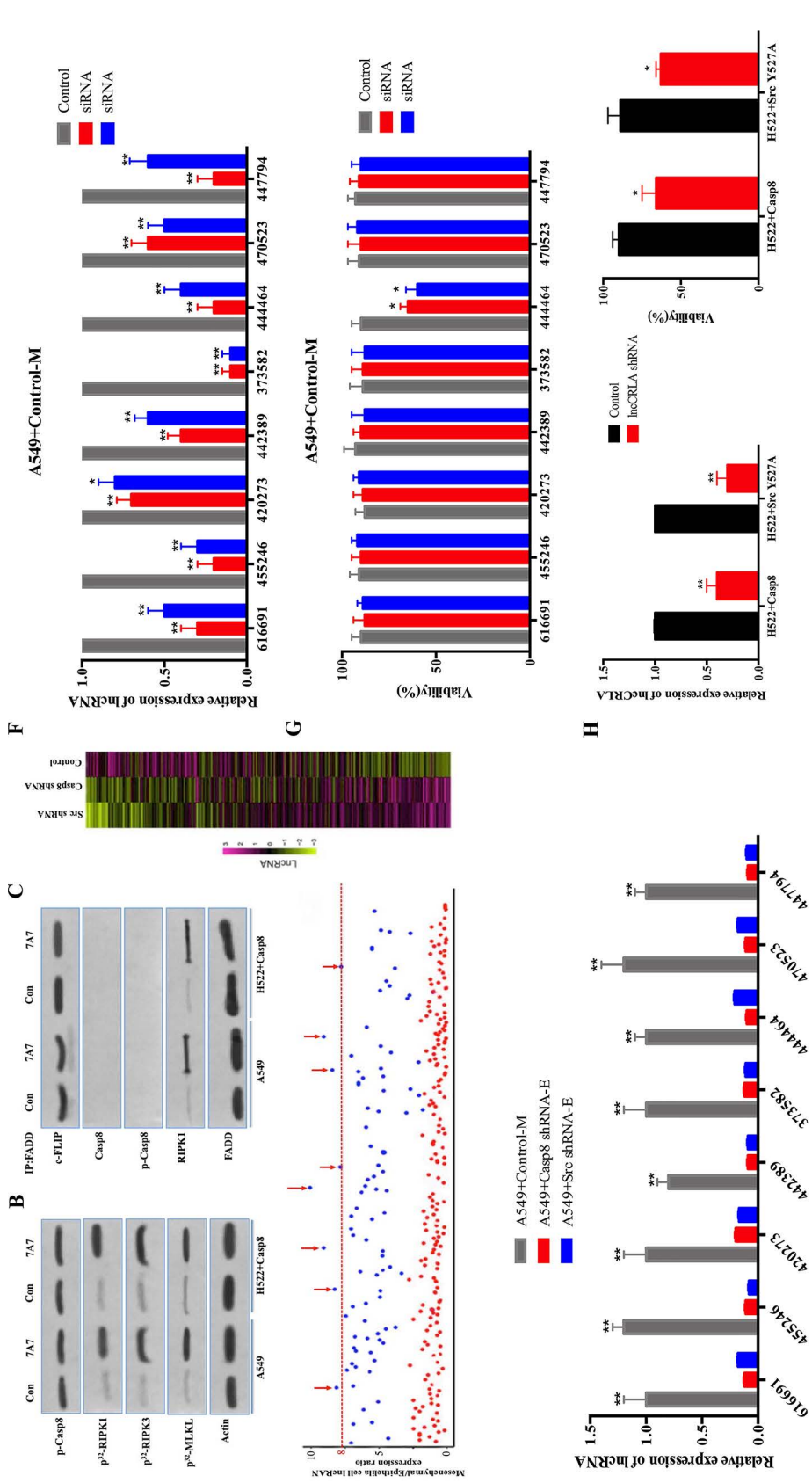

Figure 5. lncRNA-related chemotherapy resistance in lung adenocarcinoma (lncCRLA) inhibited RIPK1-induced necroptosis in the mesenchymal-like lung adenocarcinoma. (A) Immunoblotting analysis of p-Casp-8 and β-actin in the A549 cells and H522 cells with caspase 8 treated by 200 nM paclitaxel with or without 747 antibody for 48 h after 48-h attachment on the fibronectin-coated dish. Cells were labeled with [^{32}P]-orthophosphate. Phosphorylated RIPK1, RIPK3, and MLKL were measured by Cyclone Plus Phosphor Imager. (B) The immunocomplexes of A549 cells and H522 cells with caspase 8 treated by 200 nM paclitaxel for 48 h after 48-h attachment on the fibronectin-coated dish were eluted with antibody against FADD, and whole elution was used to measure c-FLIP, caspase 8, p-Casp8, and RIPK1. (C) lncRNA microarray data of the mesenchymal-like (A549 + control) and the epithelial-like (A549 + c-Src/caspase 8 shRNA) cells were presented in a heatmap. (D) Most differently expressed lncRNAs between mesenchymal-like (A549 + control) and epithelial-like (A549 + c-Src/caspase 8 shRNA) cells based on lncRNA microarray, >8-fold. (E) Verification of indicated lncRNAs in the mesenchymal-like (M) or epithelial-like (E) A549 cells by quantitative reverse transcription polymerase chain reaction (qRT-PCR) ($n = 3$). (F) Verification of interference efficiency of siRNAs for indicated lncRNAs in A549 cells with control shRNA by qRT-PCR ($n = 3$). (G) A549 cells with control shRNA transfected with indicated siRNAs were treated with 200 nM paclitaxel for 48 h after 48-h attachment on the fibronectin-coated dish. Cell viability was determined by measuring ATP levels using Cell Titer-Glo kit. Data were represented as mean ± standard deviation of duplicates. *p< 0.05 versus control. (H) qRT-PCR analysis of lncCRLA in H522 cells with c-Src Y527F/caspase 8 stably transfected with control or lncCRLA shRNA (left). Tumor cells as indicated were treated with 200 nM paclitaxel for 48 h. Cell viability was determined by measuring ATP levels using Cell Titer-Glo kit (right). Data were represented as mean ± standard deviation of duplicates. * $p < 0.05$ versus control. **$p < 0.01$ versus control.

cells (Fig. 5E and Fig. S5C). The selected lncRNAs were then subjected to loss-of-function and gain-of-function analyses in the mesenchymal-like and the epithelial-like cells, respectively (Fig. S5D and E). In the mesenchymal-like A549 cells (A549 + control), of the eight most differentially expressed lncRNAs, lncRNA 444464 was the only one to increase the sensitivity to paclitaxel when knocked down (Fig. 5F and G). Notably, lncRNA 444464 failed to rescue paclitaxel-induced death of A549 + c-Src shRNA cells (Fig. S5F), but was able to obviously decrease paclitaxel-induced death of A549 + caspase 8 shRNA cells (Fig. S5G). Therefore, we focused on the uncharacterized lncRNA 444464 (*ENST00000444464*) and named it lncRNA-related chemotherapy resistance in lung adenocarcinoma (lncCRLA). This long-coding RNA was located on chromosome 17 in humans and 512 nucleotides (nt) in length (Fig. S5H). The noncoding nature of lncCRLA was confirmed by coding potential analysis (Fig. S5I). Consistently, the mesenchymal-like H522 cells (H522 + Src Y527F/caspase 8: mesenchymal) had a much higher level of lncCRLA than the epithelial-like H522 cells (H522 + control: epithelial) (Fig. S5J), and transduction of lncCRLA shRNA efficiently enhanced cell death (Fig. 5H). We transfected exogenous lncCRLA into H522 cells, which led to a reduction in cell death (Fig. S5K). To dissect the functional role of lncCRLA, we stably overexpressed lncCRLA in caspase 8-lacking epithelial-like cells via adenoviral transduction and stably knocked down lncCRLA in the p-Casp8-positive mesenchymal-like cells via lentiviral shRNA. lncCRLA blocked RIPK1-induced necroptotic signaling and reduced the number of PI-positive cells in mesenchymal-like A549 and H522 cells (Fig. 5I). In the epithelial-like tumor cells, lncCRLA conferred resistance to paclitaxel-induced necroptosis (Fig. S5L). Taken together, these data indicated that lncCRLA efficiently hampered paclitaxel-induced necroptotic cell death but did not affect paclitaxel-induced apoptotic cell death in lung adenocarcinoma.

We sought to determine how lncCRLA influenced paclitaxel-induced necroptosis. lncCRLA was predominantly located in the cytoplasm of A549 + control cells (Fig. S5M). lncCRLA might function as a competing endogenous RNA to sequester microRNAs (miRNAs), leading to the liberation of corresponding miRNA-targeted transcripts. Subsequent bioinformatics analysis by TargetScan and miRanda showed no putative miRNA response elements. How did lncCRLA impair paclitaxel-mediated RIPK1-induced necroptosis? The radioimmunoprecipitation (RIP) assay showed that lncCRLA interacts with RIPK1 but not RIPK3 in paclitaxel-treated mesenchymal-like tumor cells (Fig. 5J and Fig. S5N). The RNA pull-down assay confirmed the interaction between RIPK1 and lncCRLA in H522 cells with ectopic lncCRLA expression (Fig. S5O). To validate the target domain of RIPK1 for lncCRLA, truncated RIPK1 constructs were created with HA tag (Fig. S5P) and stably transfected into the lncCRLA-expressing H522 cells with RIPK1 knockdown via adenoviral shRNA. The functional role of lncCRLA was determined by its binding to the ID of RIPK1 independent of the KD and DD (Fig. S5P). It was reasonable that binding of RIPK1 to lncCRLA blocked the RHIM of RIPK1, leading to the inability of RIPK3 to interact with the RHIM of RIPK1 to elicit resistance to paclitaxel in lung adenocarcinoma.

We investigated how lncCRLA was upregulated in the mesenchymal-like lung adenocarcinoma cells. Our previous study revealed that the transcriptional activity of transcription factor 4 (TCF-4) was predominant in inducing the EMT phenotype in lung adenocarcinoma[17]. We hypothesized that TCF-4 functioned as a transcription factor to upregulate lncCRLA. After the promoter region of lncCRLA was reviewed, two Wnt-responsive elements (WRE) were detected between –286 and –292 (5′-CTTTGTG-3′) and between –96 and −102 of the transcription start site (TSS) (5′-CTTTGGC-3′). We constructed a set of lncCRLA promoters linked to a luciferase reporter in the mesenchymal-like tumor cells. As shown in Figure 5K, the lncCRLA promoter was able to markedly increase the luciferase activity in the mesenchymal-like lung adenocarcinoma cells, which was confirmed by chromatin immunoprecipitation (ChIP) assay using an antibody specific for TCF-4 (Fig. S5Q).

We next investigated lncCRLA expression and the relationship between lncCRLA and chemotherapy response in patients with lung adenocarcinoma. lncCRLA expression was determined by locked nucleic acid (LNA)-based in situ hybridization (ISH) (Fig. 5L) and was significantly increased in patients with resectable and metastatic lung adenocarcinoma who had progressive disease (PD) (Fig. 5M and Fig. S5R). Moreover, lncCRLA expression was positively correlated with p-Casp8 expression (Fig. S5S). Lower lncCRLA produced a marked benefit for PFS in the patients with resectable lung adenocarcinoma (Fig. S5T). Taken together, these data suggested that upregulation of lncCRLA enhanced chemotherapy resistance of the mesenchymal-like lung adenocarcinoma to paclitaxel by directly binding to RIPK1 to block necroptosis.

c-Src Inhibitor, Dasatinib, and c-FLIP Knockdown Sensitized the Mesenchymal-Like Lung Adenocarcinoma Cells to Paclitaxel-Induced Cytotoxicity

The prior results indicated that c-Src overactivation via its interaction with phosphorylated caspase 8 triggered EMT to yield a limited benefit for paclitaxel treatment[17]. Hence, we determined whether the c-Src inhibitor, dasatinib, could increase the therapeutic benefit of paclitaxel through EMT blockade and caspase 8 dephosphorylation.

Dasatinib was capable of ablating the effects of caspase 8 phosphorylation and c-Src activation in A549 + control and H522 + caspase 8 (Fig. 6A), in which dasatinib efficiently blocked the EMT phenotype and lncCRLA expression (Fig. S6A–C). Dasatinib sensitized lung adenocarcinoma cells to paclitaxel (Fig. 6B). Surprisingly, the proportion of PI-positive cells increased by approximately 30% in cells treated with paclitaxel plus dasatinib (Fig. 6C), while the proportion of annexin V-positive cells was comparable among the various cell lines (Fig. 6C). The contribution of dasatinib to the therapeutic efficacy of paclitaxel in lung adenocarcinoma was confirmed by an in vivo xenograft experiment (Fig. 6D and E). Consistently, dasatinib enhanced necroptosis by activating RIPK1/RIPK3/MLKL but did not enhance the apoptotic cleavage of caspase 8 in the mesenchymal-like A549 and H522 cells when combined with paclitaxel (Fig. 6F).

Subsequently, we investigated why caspase 8 dephosphorylation via dasatinib-induced c-Src inactivation did not lead to apoptotic cell death. It was noteworthy that in the paclitaxel-treated A549 and H522 cells, dephosphorylated caspase 8 induced by dasatinib did not coimmunoprecipitate with FADD, while c-FLIP, an inhibitor of caspase 8-induced apoptosis, predominantly bound to FADD independent of dasatinib addition (Fig. S6D). The interaction between RIPK1 and FADD was strengthened by the addition of dasatinib (Fig. S6D). It was more likely that blocking phosphorylated caspase 8 from binding FADD accounted for the mechanism by which dasatinib-mediated dephosphorylated caspase 8 could not bind FADD due to c-FLIP occupying the binding pocket.

To explore the influence of c-FLIP on the sensitivity of lung adenocarcinoma to paclitaxel and dasatinib, we constructed five siRNAs targeting c-FLIP. According to knockdown efficiency of the siRNAs in A549 + control and H522 + caspase 8 (Fig. S6E and F), we selected siRNA2 and siRNA4 to construct lentiviral shRNA1 and shRNA2 stably transfected into tumor cells. c-FLIP knockdown markedly promoted the apoptosis of A549 and H522 cells treated with dasatinib plus paclitaxel (Fig. 6G, and Fig. S6G and H). c-FLIP knockdown did not affect RIPK1 activation, but caspase 8 was recruited to FADD and apoptotically cleaved in both cell lines, in which shRNA1 and shRNA2 of c-FLIP yielded similar effects with different knockdown levels of c-FLIP (Fig. S6I and J). Intriguingly, both c-FLIP shRNA1 and shRNA2 similarly facilitated apoptosis in the A549 + c-Src shRNA treated with paclitaxel (Fig. S6K and L). c-FLIP knockdown by shRNA2 suppressed tumor growth in A549 cells with control shRNA and H522 cells with caspase 8 in in vivo xenograft experiments (Fig. 6H). We observed that c-FLIP shRNA2 did not restrict the therapeutic benefit with a lesser attenuation in c-FLIP expression compared with c-FLIP shRNA1, suggesting that a reduction in c-FLIP expression to some extent was sufficient to sensitize the paclitaxel + dasatinib treatment in lung adenocarcinoma.

We tested the possibility of delivering siRNA targeting c-FLIP combined with paclitaxel liposomes. The paclitaxel liposome plus c-FLIP siRNA (siFLIP) was constructed on the basis of paclitaxel liposomes as a common pharmacological delivery mechanism (Fig. 6I). As shown in Figure S6M, paclitaxel liposomes had a great potential to transduce siFLIP into A549 cells. Paclitaxel liposome + siFLIP reduced the mRNA and protein levels of c-FLIP in the mesenchymal-like A549 + control and H522 + caspase 8 cells (Fig. 6J and Fig. S6N), while paclitaxel liposome + siFLIP combined with dasatinib predominantly eliminated tumor cells in vivo and in vitro (Fig. S6O and P). We then established a patient-derived xenograft (PDX) model to determine the response of lung adenocarcinoma to the combination of paclitaxel liposome + siFLIP and dasatinib. To adequately utilize the patient-derived sample, a PDX model was designed and illustrated in Figure S6Q, and patients involved in the PDX experiment are listed in Table S4. Accordingly, paclitaxel liposome + siFLIP plus dasatinib was significantly superior in inhibiting the growth of tumor cells from patients with resectable lung adenocarcinoma compared with other treatments (Fig. 6K and Fig. S6R). Collectively, c-FLIP knockdown was able to sensitize the mesenchymal-like lung adenocarcinoma to dual therapies of paclitaxel plus dasatinib.

DISCUSSION

During the process of becoming more invasive and motile, cancer cells that have undergone EMT also acquire resistance to several drugs and chemotherapeutic agents[6]. Our prior work showed that the c-Src–caspase 8 interaction was able to specifically phosphorylate caspase 8 at tyrosine 380 and overactivate c-Src to facilitate EMT[16]. We generalized our notion that EMT occurred when c-Src-mediated phosphorylation of caspase 8 overactivated c-Src in a positive feedback loop. It was of major interest that caspase 8 phosphorylation was ascribed to c-Src expression level in lung adenocarcinoma. Although c-Src is activated by multiple growth and metastatic signaling pathways[25], we determined that phosphorylated caspase 8 by c-Src played a key role in overactivating c-Src to trigger EMT in lung adenocarcinoma. Our team has focused on the basic activation of c-Src prior to caspase 8 phosphorylation (data unpublished). Multiple EMT factors and EMT signaling are more pronounced in cancer tissues[26,27]. Although a plethora of biomarkers have been utilized in the EMT process, Vim and E-cad are the best markers in lung adenocarcinoma[15]. We found that p-Casp8-expressing lung adenocarcinoma tissues had the propensity to present with a mesenchymal phenotype with downregulated E-cad and upregulated Vim and corresponded to a lower response rate to treatment

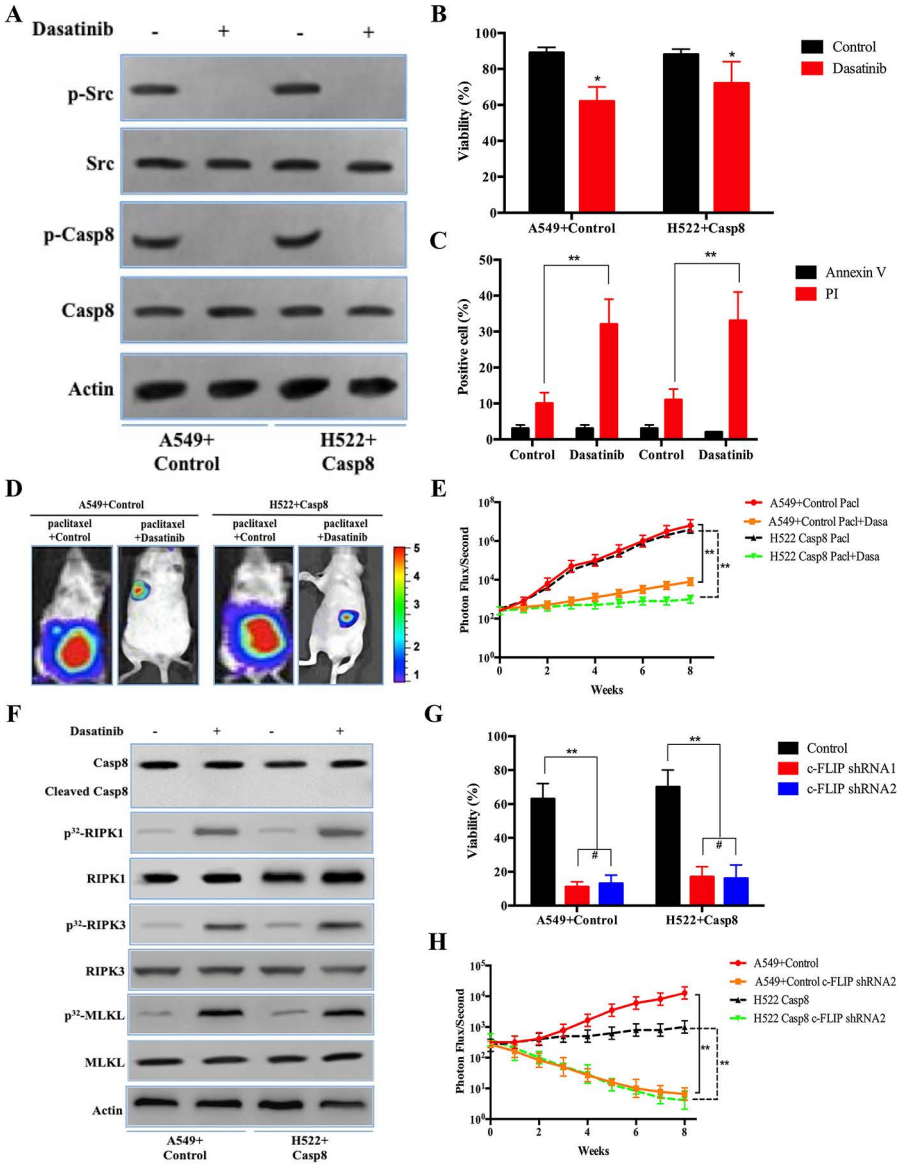

Figure 6. c-Src inhibitor, dasatinib, and c-FLIP knockdown sensitized the mesenchymal-like lung adenocarcinoma cells to paclitaxel-induced cytotoxicity. (A) Immunoblotting analysis of p-Src, c-Src, p-Casp8, caspase 8, and β-actin in the A549 cells with control shRNA and H522 cells with caspase 8 treated by 200 nM paclitaxel for 48 h after 48-h attachment on the fibronectin-coated dish. (B) A549 cells with control shRNA and H522 cells with caspase 8 were treated with 200 nM paclitaxel combined with or without dasatinib (20 nM) for 48 h after 48-h attachment on the fibronectin-coated dish. Cell viability was determined by measuring ATP levels using Cell Titer-Glo kit. Data were represented as mean ± standard deviation of duplicates. $*p < 0.05$ versus control. (C) A549 cells with control shRNA and H522 cells with caspase 8 were treated with 200 nM paclitaxel combined with or without dasatinib (20 nM) for 48 h after 48-h attachment on the fibronectin-coated dish. Cells were analyzed for annexin V/PI staining by flow cytometry. All experiments were repeated three times with similar results. $**p < 0.01$ versus control. (D, E) Nude mice were subcutaneously xenografted with A549 cells with control shRNA and H522 cells with caspase 8 (1.0×10^6 cells) treated intravenously with paclitaxel plus oral vector or dasatinib ($n = 5$ per group). Representative bioluminescence images (D), quantification of bioluminescence imaging signal intensities (E). $**p < 0.01$ versus control. (F) Immunoblotting analysis of caspase 8, cleaved caspase 8, RIPK1, RIPK3, MLKL, and β-actin in the A549 cells with control shRNA and H522 cells with caspase 8 treated by 200 nM paclitaxel combined with or without dasatinib (20 nM) for 48 h after 48-h attachment on the fibronectin-coated dish. (G) A549 cells with control shRNA and H522 cells with caspase 8 stably transfected with control shRNA, c-FLIP shRNA1, and c-FLIP shRNA2 were treated with 200 nM paclitaxel combined with or without dasatinib (20 nM) for 48 h after 48-h attachment on the fibronectin-coated dish. Cell viability was determined by measuring ATP levels using Cell Titer-Glo kit. Data were represented as mean ± standard deviation of duplicates. $**p < 0.01$ versus control. (H) Nude mice were subcutaneously xenografted with A549 cells with control shRNA and H522 cells with caspase 8 stably transfected by c-FLIP shRNA2 (1.0×10^6 cells) treated with paclitaxel plus dasatinib ($n = 5$ per group). Quantification of bioluminescence imaging signal intensities. $**p < 0.01$ versus control.

and a worse 5-year PFS. It was rationalized that p-Casp8 was responsible for disease progression arising from the EMT phenotype and chemoresistance in patients with lung adenocarcinoma.

Combined paclitaxel and cisplatin has been the cornerstone for NSCLC treatment for many years. Both drugs have completely different mechanisms in eliminating cancer cells[28]. p53 plays a central role in cisplatin-induced cell death[29]. Consistently, our results unveiled that cisplatin killed lung adenocarcinoma cells independent of caspase 8 and c-Src. In parallel, paclitaxel increased mitotic arrest regardless of caspase 8 or c-Src as well as markedly induced cell death in a caspase 8-dependent manner. Thus, we sought to determine whether p-Casp8 might be the lynchpin for EMT-related chemoresistance.

Necroptosis was observed to be a compensatory mechanism under the condition of apoptotic blockade[30,31]. We detected that phosphorylating caspase 8 by c-Src or silencing caspase 8 rescued numerous lung adenocarcinoma cells from death, but failed to prevent 10%–30% necroptotic cell death from paclitaxel. These results implied that caspase 8 phosphorylation or silencing yielded resistance to paclitaxel due to apoptotic inhibition. Traditionally, paclitaxel, an antimitotic drug, disrupts spindle assembly leading to mitotic arrest by persistent activation of the spindle assembly checkpoint (SAC). Following prolonged arrest, cells either die in mitosis or undergo ''slippage,'' returning to interphase without completing cell division[32,33]. More recently, mitotic arrest was reported to lead to DNA damage and genetic instability, which does not give rise to a large number of cell deaths[34,35]. Our results showed that paclitaxel increased the proportion of cells in mitotic arrest independently of caspase 8 corresponding to a disproportionately increased amount of cell death dependently of caspase 8. Therefore, paclitaxel-induced mitotic arrest can be distinguished from its tumoricidal function.

FADD, caspase 8, and c-FLIP inhibited necroptosis by suppressing RIPK1 and RIPK3 within this complex[36], while FADD–caspase 8–c-FLIP complex inhibition resulted in the FADD-induced assembly of the RIPK1–RIPK3 complex for necroptosis[37,38]. The assembly of the RIPK1–RIPK3 complex via RHIM in response to a variety of stimuli was critical to initiate RIPK1 phosphorylation, which was required for RIPK3–RIPK3 dimerization and RIPK3 phosphorylation, eventually resulting in MLKL phosphorylation to trigger necroptosis[39,40]. It was approved by our observation that FADD was required to recruit RIPK1 leading to necroptosis and caspase 8 to induce apoptosis following paclitaxel treatment. These results indicated that FADD functioned as a sensor for cell death stimuli under paclitaxel treatment.

The FADD–c-FLIP complex in the absence of caspase 8 and RIPK1 existed under no treatment. Under paclitaxel stimulation, caspase 8 replaced c-FLIP and interacted with FADD-involved complex to trigger apoptosis in lung adenocarcinoma cells with unphosphorylated caspase 8. It was hypothesized that caspase 8 possesses a higher affinity to FADD relative to c-FLIP under apoptotic stimuli. Caspase 8–c-FLIP based on FADD was reported to inhibit necroptosis by cleaving RIPK1 (at D324) and RIPK3 (at D333) within this complex[37]. Nevertheless, RIPK1 and RIPK3 showed similar expression levels before and after paclitaxel treatment. We found that RIPK1-induced necroptosis was undetectable with the onset of apoptosis in the paclitaxel-treated A549 cells with c-Src shRNA. It was postulated that apoptosis still counteracted RIPK1-induced necroptosis by restricting RIPK1 involvement instead of cleaving RIPK1. It was intriguing that knockdown of c-FLIP did not enhance A549 and H522 cell death with paclitaxel treatment. This was attributed to two mechanisms: c-FLIP was replaced by caspase 8 under apoptotic conditions, while c-FLIP had no influence on necroptosis under necroptotic conditions.

Although caspase 8 phosphorylation and caspase 8 deficiency impaired apoptosis under paclitaxel treatment, caspase 8 phosphorylation induced a smaller amount of necroptotic death than did caspase 8 deficiency. Caspase 8 phosphorylation by c-Src initiated EMT to protect tumor cells from paclitaxel-induced antitumor activity. This notion was supported by the observation that compared with the mesenchymal-like A549 cells with control shRNA, the epithelial-like A549 cells with RNF43 shRNA presenting c-Src–caspase 8 interaction had a higher proportion of cells killed via paclitaxel-induced necroptosis. We focused on the contribution of lncRNAs to the resistance of lung adenocarcinoma to paclitaxel. After lncRNA microarray profiling, lncCRLA had the most outstanding effects on the resistance to paclitaxel in the mesenchymal-like lung adenocarcinoma by binding to the ID of RIPK1 to interfere with RIPK1–RIPK3 interaction-based necroptosis. The RHIM domain in the ID of RIPK1 was blocked to hamper its interaction with RIKP3. In addition, exogenous lncCRLA expression rescued the caspase 8-deficient epithelial-like lung adenocarcinoma from necroptosis.

Dasatinib has been characterized as one of the most efficient antagonists for c-Src and has been recently approved for clinical use in acute lymphoblastic leukemia and several solid tumors[41,42]. Dasatinib did not increase apoptotic cell death through caspase 8 cleavage but increased necroptosis in lung adenocarcinoma. Mechanistically, FADD was excessively occupied by c-FLIP in cells with caspase 8 phosphorylation, but phosphorylated caspase 8 was dissociated from FADD under paclitaxel treatment. Therefore, caspase 8 dephosphorylation could not trigger apoptotic cleavage due to dephosphorylated caspase 8 dissociated from FADD. On the other hand, dasatinib facilitated necroptosis by blocking

EMT and suppressing lncCRLA expression. We expected the activation of apoptosis and necroptosis to significantly increase antitumor effects in the mesenchymal-like lung adenocarcinoma with p-Casp8. Our team collaborated with the Lv Ye pharmacy to create paclitaxel liposomes encapsulating siFLIP, which had been verified to function as a strong antitumor agent and combined these liposomes with dasatinib to treat the mesenchymal-like lung adenocarcinoma. It was noteworthy that c-FLIP knockdown to a lesser extent was sufficient to initiate apoptotic function of caspase 8.

CONCLUSIONS

c-Src mediated caspase 8 phosphorylation, which is essential for the EMT phenotype through c-Src overactivation in lung adenocarcinoma cell lines. The shift of these cells to the mesenchymal phenotype leads to chemoresistance to cisplatin plus paclitaxel in patients with resectable lung adenocarcinoma, who also have a significantly worse 5-year PFS rate. Cisplatin killed lung adenocarcinoma cells independent of caspase 8 status, while paclitaxel triggered necroptosis in lung adenocarcinoma cells with caspase 8 phosphorylation or deficiency,

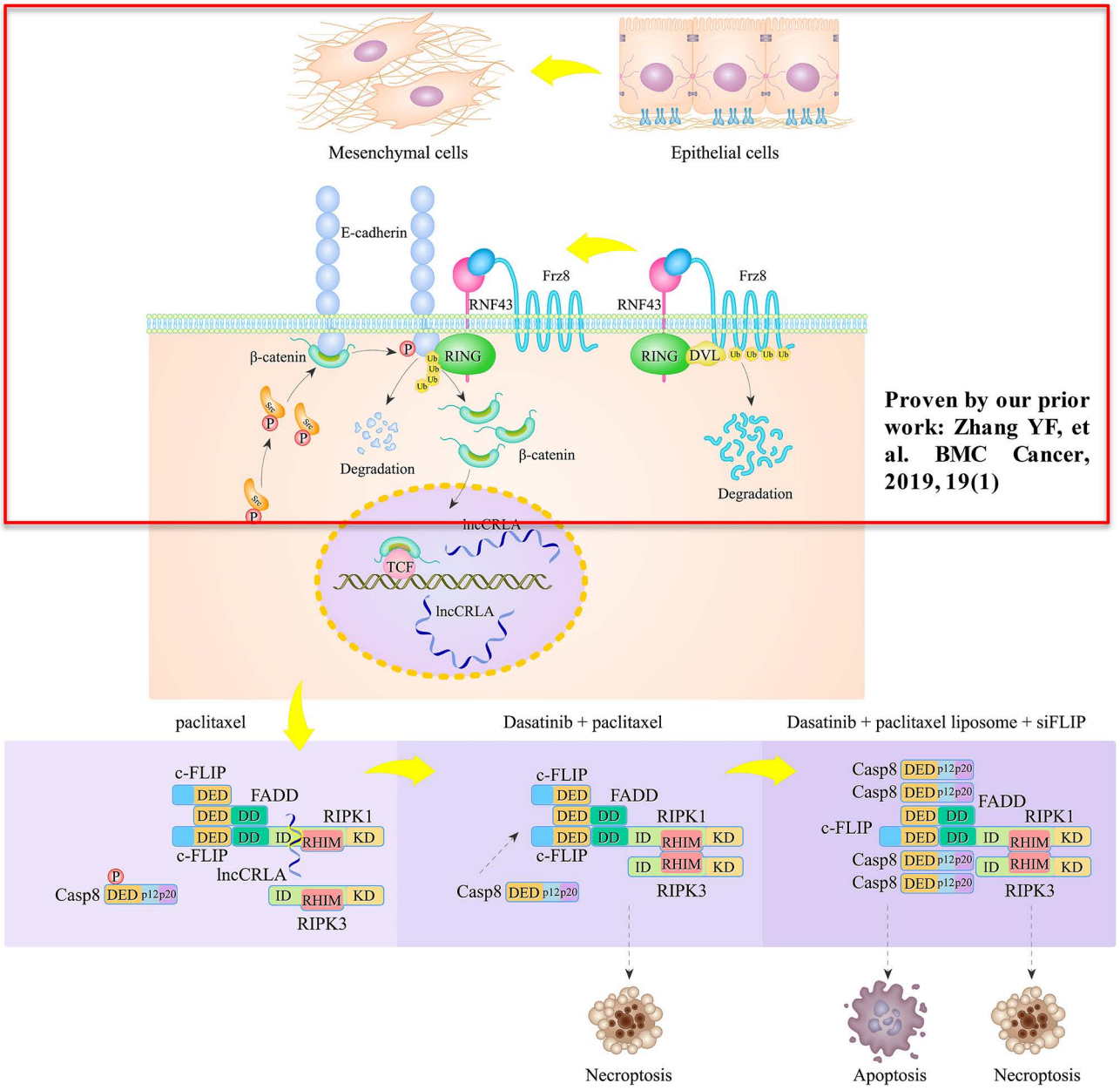

Figure 7. A schematic diagram of the resistance of the mesenchymal-like lung adenocarcinoma cells to paclitaxel.

during which FADD interacted with RIPK1 via the DD to block RIPK1/RIPK3/MLKL signaling. Furthermore, a brand-new lncRNA, named lncCRLA, was significantly upregulated by TCF-4 and inhibited RIPK1-induced necroptosis in the mesenchymal-like lung adenocarcinoma cells by impairing of RIPK1–RIPK3 interaction via binding to the ID of RIPK1. Dasatinib enhanced necroptosis in paclitaxel-treated lung adenocarcinoma cells that underwent EMT, while c-FLIP knockdown predominantly sensitized mesenchymal-like lung adenocarcinoma to dasatinib + paclitaxel through apoptosis. Together, the c-Src–caspase 8 interaction initiated the EMT phenotype and chemoresistance by caspase 8 phosphorylation and chemoresistance-related lncRNA expression, to which treatment with dasatinib plus paclitaxel liposome + siFLIP was lethal (Fig. 7).

ACKNOWLEDGMENTS: *This study was supported by the National Natural Science Foundation of China (Nos. 81301847 and 81872390). Author contributions: conception and design: Yang Zhao; administrative support: Shuqun Zhang and Weili Min; provision of study materials or patients: Yang Zhao, Liangzhang Sun, Xiao Gao, Xiao Gao, Weili Min, and Burong Li; collection and assembly of data: Yang Zhao, Liangzhang Sun, and Xiao Gao; manuscript writing: Yang Zhao; and final approval of manuscript: Yang Zhao. All authors approved the manuscript for publication. All data and materials are available when required. Supplementary material link: Our supplementary files including Figures S1–S6 and Tables S1–S4 and supplementary materials are accessible by link https://pan.baidu.com/s/1tIjpWffR7vppC6kOH_62nQ (password: zthj). The authors declare no conflicts of interest.*

REFERENCES

1. Siegel RL, Miller KD, Jemal A. Cancer statistics, 2018. CA Cancer J Clin. 2018;68(1):7–30.
2. Zheng R, Zeng H, Zuo T, Zhang S, Qiao Y, Zhou Q, Chen W. Lung cancer incidence and mortality in China, 2011. Thorac Cancer 2016;7(1):94–99.
3. Oxnard GR, Binder A, Janne PA. New targetable oncogenes in non-small-cell lung cancer. J Clin Oncol. 2013;31(8):1097–1104.
4. Jamal-Hanjani M, Wilson GA, McGranahan N, Birkbak NJ, Watkins TBK, Veeriah S, Shafi S, Johnson DH, Mitter R, Rosenthal R, Salm M, Horswell S, Escudero M, Matthews N, Rowan A, Chambers T, Moore DA, Turajlic S, Xu H, Lee SM, Forster MD, Ahmad T, Hiley CT, Abbosh C, Falzon M, Borg E, Marafioti T, Lawrence D, Hayward M, Kolvekar S, Panagiotopoulos N, Janes SM, Thakrar R, Ahmed A, Blackhall F, Summers Y, Shah R, Joseph L, Quinn AM, Crosbie PA, Naidu B, Middleton G, Langman G, Trotter S, Nicolson M, Remmen H, Kerr K, Chetty M, Gomersall L, Fennell DA, Nakas A, Rathinam S, Anand G, Khan S, Russell P, Ezhil V, Ismail B, Irvin-Sellers M, Prakash V, Lester JF, Kornaszewska M, Attanoos R, Adams H, Davies H, Dentro S, Taniere P, O'Sullivan B, Lowe HL, Hartley JA, Iles N, Bell H, Ngai Y, Shaw JA, Herrero J, Szallasi Z, Schwarz RF, Stewart A, Quezada SA, Le Quesne J, Van Loo P, Dive C, Hackshaw A, Swanton C, Consortium TR. Tracking the evolution of non-small-cell lung cancer. N Engl J Med. 2017;376(22):2109–2121.
5. Herbst RS, Morgensztern D, Boshoff C. The biology and management of non-small cell lung cancer. Nature 2018;553(7689):446–454.
6. Fischer KR, Durrans A, Lee S, Sheng J, Li F, Wong ST, Choi H, El Rayes T, Ryu S, Troeger J, Schwabe RF, Vahdat LT, Altorki NK, Mittal V, Gao D. Epithelial-to-mesenchymal transition is not required for lung metastasis but contributes to chemoresistance. Nature 2015;527(7579):472–476.
7. Chang A. Chemotherapy, chemoresistance and the changing treatment landscape for NSCLC. Lung Cancer 2011;71(1):3–10.
8. Brabletz T. EMT and MET in metastasis: Where are the cancer stem cells? Cancer Cell 2012;22(6):699–701.
9. Thiery JP, Lim CT. Tumor dissemination: An EMT affair. Cancer Cell 2013;23(3):272–273.
10. Tsai JH, Donaher JL, Murphy DA, Chau S, Yang J. Spatiotemporal regulation of epithelial–mesenchymal transition is essential for squamous cell carcinoma metastasis. Cancer Cell 2012;22(6):725–736.
11. Kalluri R, Weinberg RA. The basics of epithelial–mesenchymal transition. J Clin Invest. 2009;119(6):1420–1428.
12. Seton-Rogers S. Epithelial–mesenchymal transition: Untangling EMT's functions. Nat Rev Cancer 2016; 16(1):1.
13. Zheng X, Carstens JL, Kim J, Scheible M, Kaye J, Sugimoto H, Wu CC, LeBleu VS, Kalluri R. Epithelial-to-mesenchymal transition is dispensable for metastasis but induces chemoresistance in pancreatic cancer. Nature 2015;527(7579):525–530.
14. Diao Y, Ma X, Min W, Lin S, Kang H, Dai Z, Wang X, Zhao Y. Dasatinib promotes paclitaxel-induced necroptosis in lung adenocarcinoma with phosphorylated caspase-8 by c-Src. Cancer Lett. 2016;379(1):12–23.
15. Schliekelman MJ, Taguchi A, Zhu J, Dai X, Rodriguez J, Celiktas M, Zhang Q, Chin A, Wong CH, Wang H, McFerrin L, Selamat SA, Yang C, Kroh EM, Garg KS, Behrens C, Gazdar AF, Laird-Offringa IA, Tewari M, Wistuba, II, Thiery JP, Hanash SM. Molecular portraits of epithelial, mesenchymal, and hybrid states in lung adenocarcinoma and their relevance to survival. Cancer Res. 2015;75(9):1789–1800.
16. Cursi S, Rufini A, Stagni V, Condo I, Matafora V, Bachi A, Bonifazi AP, Coppola L, Superti-Furga G, Testi R, Barila D. Src kinase phosphorylates caspase-8 on Tyr380: A novel mechanism of apoptosis suppression. EMBO J. 2006;25(9):1895–1905.
17. Zhang Y, Sun L, Gao X, Guo A, Diao Y, Zhao Y. RNF43 ubiquitinates and degrades phosphorylated E-cadherin by c-Src to facilitate epithelial–mesenchymal transition in lung adenocarcinoma. BMC Cancer 2019;19(1):670.
18. Wei W, Birrer MJ. Spleen tyrosine kinase confers paclitaxel resistance in ovarian cancer. Cancer Cell 2015;28(1):7–9.
19. Linkermann A, Green DR. Necroptosis. N Engl J Med. 2014;370(5):455–465.
20. Wang L, Du F, Wang X. TNF-alpha induces two distinct caspase-8 activation pathways. Cell 2008;133(4):693–703.
21. Yu Y, Gaillard S, Phillip JM, Huang TC, Pinto SM, Tessarollo NG, Zhang Z, Pandey A, Wirtz D, Ayhan A, Davidson B, Wang TL, Shih Ie M. Inhibition of spleen tyrosine kinase potentiates paclitaxel-induced cytotoxicity in ovarian cancer cells by stabilizing microtubules. Cancer Cell 2015;28(1):82–96.
22. Boege Y, Malehmir M, Healy ME, Bettermann K, Lorentzen A, Vucur M, Ahuja AK, Bohm F, Mertens JC,

Shimizu Y, Frick L, Remouchamps C, Mutreja K, Kahne T, Sundaravinayagam D, Wolf MJ, Rehrauer H, Koppe C, Speicher T, Padrissa-Altes S, Maire R, Schattenberg JM, Jeong JS, Liu L, Zwirner S, Boger R, Huser N, Davis RJ, Mullhaupt B, Moch H, Schulze-Bergkamen H, Clavien PA, Werner S, Borsig L, Luther SA, Jost PJ, Weinlich R, Unger K, Behrens A, Hillert L, Dillon C, Di Virgilio M, Wallach D, Dejardin E, Zender L, Naumann M, Walczak H, Green DR, Lopes M, Lavrik I, Luedde T, Heikenwalder M, Weber A. A dual role of caspase-8 in triggering and sensing proliferation-associated DNA damage, a key determinant of liver cancer development. Cancer Cell 2017;32(3):342–359 e10.

23. Qu L, Ding J, Chen C, Wu ZJ, Liu B, Gao Y, Chen W, Liu F, Sun W, Li XF, Wang X, Wang Y, Xu ZY, Gao L, Yang Q, Xu B, Li YM, Fang ZY, Xu ZP, Bao Y, Wu DS, Miao X, Sun HY, Sun YH, Wang HY, Wang LH. Exosome-transmitted lncARSR promotes sunitinib resistance in renal cancer by acting as a competing endogenous RNA. Cancer Cell 2016;29(5):653–668.
24. Yan X, Hu Z, Feng Y, Hu X, Yuan J, Zhao SD, Zhang Y, Yang L, Shan W, He Q, Fan L, Kandalaft LE, Tanyi JL, Li C, Yuan CX, Zhang D, Yuan H, Hua K, Lu Y, Katsaros D, Huang Q, Montone K, Fan Y, Coukos G, Boyd J, Sood AK, Rebbeck T, Mills GB, Dang CV, Zhang L. Comprehensive genomic characterization of long non-coding RNAs across human cancers. Cancer Cell 2015;28(4):529–540.
25. Boumahdi S, de Sauvage FJ. The great escape: Tumour cell plasticity in resistance to targeted therapy. Nat Rev Drug Discov. 2020;19(1):39–56.
26. Lu W, Kang Y. Epithelial–mesenchymal plasticity in cancer progression and metastasis. Dev Cell 2019;49(3):361–74.
27. Aiello NM, Kang Y. Context-dependent EMT programs in cancer metastasis. J Exp Med. 2019;216(5):1016–1026.
28. Di Maio M, Chiodini P, Georgoulias V, Hatzidaki D, Takeda K, Wachters FM, Gebbia V, Smit EF, Morabito A, Gallo C, Perrone F, Gridelli C. Meta-analysis of single-agent chemotherapy compared with combination chemotherapy as second-line treatment of advanced non-small-cell lung cancer. J Clin Oncol. 2009;27(11):1836–1843.
29. Galluzzi L, Vitale I, Michels J, Brenner C, Szabadkai G, Harel-Bellan A, Castedo M, Kroemer G. Systems biology of cisplatin resistance: Past, present and future. Cell Death Dis. 2014;5:e1257.
30. Galluzzi L, Kroemer G. Necroptosis: A specialized pathway of programmed necrosis. Cell 2008;135(7):1161–1163.
31. Zhou W, Yuan J. SnapShot: Necroptosis. Cell 2014;158(2):464–464 e1.
32. Gulluni F, Martini M, De Santis MC, Campa CC, Ghigo A, Margaria JP, Ciraolo E, Franco I, Ala U, Annaratone L, Disalvatore D, Bertalot G, Viale G, Noatynska A, Compagno M, Sigismund S, Montemurro F, Thelen M, Fan F, Meraldi P, Marchio C, Pece S, Sapino A, Chiarle R, Di Fiore PP, Hirsch E. Mitotic spindle assembly and genomic stability in breast cancer require PI3K-C2alpha scaffolding function. Cancer Cell 2017;32(4):444–459 e7.
33. Topham C, Tighe A, Ly P, Bennett A, Sloss O, Nelson L, Ridgway RA, Huels D, Littler S, Schandl C, Sun Y, Bechi B, Procter DJ, Sansom OJ, Cleveland DW, Taylor SS. MYC is a major determinant of mitotic cell fate. Cancer Cell 2015;28(1):129–140.
34. Harding SM, Benci JL, Irianto J, Discher DE, Minn AJ, Greenberg RA. Mitotic progression following DNA damage enables pattern recognition within micronuclei. Nature 2017;548(7668):466–470.
35. Macheret M, Halazonetis TD. DNA replication stress as a hallmark of cancer. Annu Rev Pathol. 2015;10:425–448.
36. Dannappel M, Vlantis K, Kumari S, Polykratis A, Kim C, Wachsmuth L, Eftychi C, Lin J, Corona T, Hermance N, Zelic M, Kirsch P, Basic M, Bleich A, Kelliher M, Pasparakis M. RIPK1 maintains epithelial homeostasis by inhibiting apoptosis and necroptosis. Nature 2014;513(7516):90–94.
37. Moquin D, Chan FK. The molecular regulation of programmed necrotic cell injury. Trends Biochem Sci. 2010;35(8):434–441.
38. Oberst A, Green DR. It cuts both ways: Reconciling the dual roles of caspase 8 in cell death and survival. Nat Rev Mol Cell Biol. 2011;12(11):757–763.
39. Rickard JA, O'Donnell JA, Evans JM, Lalaoui N, Poh AR, Rogers T, Vince JE, Lawlor KE, Ninnis RL, Anderton H, Hall C, Spall SK, Phesse TJ, Abud HE, Cengia LH, Corbin J, Mifsud S, Di Rago L, Metcalf D, Ernst M, Dewson G, Roberts AW, Alexander WS, Murphy JM, Ekert PG, Masters SL, Vaux DL, Croker BA, Gerlic M, Silke J. RIPK1 regulates RIPK3–MLKL-driven systemic inflammation and emergency hematopoiesis. Cell 2014;157(5):1175–1188.
40. Wu XN, Yang ZH, Wang XK, Zhang Y, Wan H, Song Y, Chen X, Shao J, Han J. Distinct roles of RIP1–RIP3 hetero- and RIP3–RIP3 homo-interaction in mediating necroptosis. Cell Death Differ. 2014;21(11):1709–1720.
41. Li J, Rix U, Fang B, Bai Y, Edwards A, Colinge J, Bennett KL, Gao J, Song L, Eschrich S, Superti-Furga G, Koomen J, Haura EB. A chemical and phosphoproteomic characterization of dasatinib action in lung cancer. Nat Chem Biol. 2010;6(4):291–299.
42. Leveque D. Pharmacokinetic interactions of dasatinib and docetaxel. Lancet Oncol. 2014;15(2):e51.